

Dissociation dynamics of resonantly coupled bose-fermi mixtures in an optical lattice

Takahiko Miyakawa and Pierre Meystre

Department of Physics, The University of Arizona, Tucson, Arizona 85721, USA

(Dated: May 22, 2018)

We consider the photodissociation of ground-state bosonic molecules trapped in an optical lattice potential into a two-component gas of fermionic atoms. The system is assumed to be described by a single-band resonantly-coupled Bose-Fermi Hubbard model. We show that in the strong fermion-fermion interaction limit the dissociation dynamics is governed by a spin-boson lattice Hamiltonian. In the framework of a mean-field analysis based on a generalized Gutzwiller ansatz, we then examine the crossover of the dissociation from a regime of independent single-site dynamics to a regime of cooperative dynamics as the molecular tunneling increases. We also show that in the limits of weak and strong intersite tunneling the mean-field solutions agree well with the results from the quantum optical Jaynes-Cummings and Tavis-Cummings models, respectively. Finally, we identify two types of self-trapping transitions, a *coherent* and an *incoherent* one, depending on the ratio of the repulsive molecule-molecule interaction strength to molecular tunneling.

PACS numbers: 03.75.Ss, 05.30.Fk, 32.80Pj, 67.60.-g

I. INTRODUCTION

The formation of molecules by Feshbach resonance [1] and by two-photon Raman photoassociation [2] from ultracold atomic gases trapped in an optical lattice potential offers remarkable opportunities to study some of the long-standing questions of condensed matter physics in systems under exquisite control, and is also of much interest for quantum information science [3, 4]. External control parameters such as laser and magnetic field strengths can be controlled precisely in real time, allowing the experimental investigation of the dynamics of strongly correlated systems from the adiabatic to the sudden regime, the study of the formation of long-range order and defects as the system transits across quantum critical points, and the engineering of exotic many-body states starting from various quantum phases [5, 6].

The creation of molecules from cold atoms in optical lattices has been demonstrated experimentally by several groups. Applying two-photon Raman lasers on ^{87}Rb atoms in a 3-dimensional (3D) lattice, T. Rom *et al.* succeeded in controlling both the internal and center-of-mass states of the molecules by changing the detuning of the photoassociation laser fields [7]. Unfortunately, the molecular decay arising from the spontaneous emission induced by Raman laser photons exceeded the photoassociation coupling, so that this experiment could not observe coherent Rabi oscillations between atoms and molecules. The first lattice experiments exploiting the passage of fermions (^{40}K atoms) across a Feshbach resonance were performed by M. Köhl *et al.* [8]. They observed the occupation of atoms in higher Bloch bands near the resonance, indicating that the inclusion of interband coupling is crucial for the description of a broad Feshbach resonance in optical lattices [9]. They also created Feshbach molecules from fermionic atoms in a three-dimensional optical lattice [10], and found that the measured binding energy of the molecules is in good agreement with the theoretical predictions of single-channel

models of atoms in a tight trap [11, 12]. We also mention a recent experiment by G. Tialhammer *et al.* [13], who created long-lived $^{87}\text{Rb}_2$ molecules, with lifetimes of up to 0.7s, in a three-dimensional optical lattice via a narrow Feshbach resonance.

In a recent experiment, C. Ryu *et al.* generated a quantum degenerate gas of molecules via photoassociation of ^{87}Rb atoms, and observed a clear coherent atom-molecule oscillation in an optical lattice, with Rabi frequency $\approx 4.13\text{kHz}$ [14]. In this experiment the atoms were initially in the Mott-insulator (MI) phase. For the duration of the photoassociation pulse each atom was trapped in the ground state of a single lattice site with trapping frequency $\omega_{\text{lattice}} \approx 2\pi \times 27\text{kHz}$, and the atom-atom interaction strength and atomic intersite tunneling were of the order of $\sim 10\text{kHz}$ and $\lesssim 10\text{Hz}$, respectively. In general, the initial atomic state in that experiment can be in either the MI or the superfluid (SF) phase, depending on the depth of the optical lattice. Combined with the interplay between two-body interactions, intersite tunneling, and atom-molecule coupling, this results in the photoassociation process exhibiting a very rich dynamics.

Motivated by these experimental advances, this paper considers a gas of two-component fermionic atoms coupled to bosonic molecules via photoassociation in an optical lattice. The system consists initially of bosonic molecules only, assumed to be in a ground state corresponding to either a MI phase or a SF phase, and a cw photoassociation beam is switched on instantaneously at $t = 0$. Our goal is to study the subsequent dissociation dynamics of the bosonic molecules into fermionic atoms. We examine the crossover of the dynamics from an independent single-site regime to a cooperative regime. We also show the appearance of two types of self-trapping transitions [15, 16], which we characterize as *coherent* and *incoherent*, as the ratio of repulsive molecule-molecule interaction strength to molecular tunneling is varied.

Section II discusses our model and formulates it as a single-band resonantly coupled Bose-Fermi Hubbard model. We show that in this model the dissociation dynamics can be described by a spin-boson lattice Hamiltonian in terms of pseudo-spin formalism. In this section we also give a formulation of mean field approximation based on a generalized Gutzwiller (GW) ansatz. Section III discusses the dissociation dynamics in several limiting cases. Specifically, we show that in the weak and strong molecular tunneling limits, respectively, it can be described in terms of generalized versions of the Jaynes-Cummings and Tavis-Cummings models of quantum optics. Section IV then presents numerical results of the GW mean-field dynamics, and section VI is a summary and outlook.

II. MODEL

A. Spin-Boson lattice Hamiltonian

We consider at zero temperature a gas of fermionic atoms of mass m_f and spin $\sigma = \uparrow, \downarrow$ trapped in an optical lattice potential. The fermionic atoms can be coherently combined into bosonic molecules of mass $m_b = 2m_f$ via two-photon Raman photoassociation. The lattice lasers are adjusted in such a way that the tight binding approximation is well justified. Since in lattice photoassociation experiments the atom-molecule interaction energy is typically small compared to the trapping energies of the atoms and molecules [7, 14] (note that this is not so for the broad Feshbach resonance of ^{40}K atoms [8, 10]) the system can be described by the single-band resonantly coupled Bose-Fermi Hubbard model [17, 18, 19, 20]

$$\hat{H}_{BF} = \hat{H}_f + \hat{H}_b + \hat{V}_{bf}, \quad (1)$$

where

$$\begin{aligned} \hat{H}_f &= -\hbar J_f \sum_{\langle ij \rangle \sigma} (\hat{f}_{i\sigma}^\dagger \hat{f}_{j\sigma} + \text{H.c.}) + \hbar \omega_f \sum_{i\sigma} \hat{n}_{i\sigma}^f \\ &+ \hbar U_f \sum_i \hat{n}_{i\uparrow}^f \hat{n}_{i\downarrow}^f, \end{aligned} \quad (2)$$

$$\begin{aligned} \hat{H}_b &= -\hbar J_b \sum_{\langle ij \rangle} (\hat{b}_i^\dagger \hat{b}_j + \text{H.c.}) + \hbar (\omega_d + \omega_b) \sum_i \hat{n}_i^b \\ &+ \frac{\hbar U_b}{2} \sum_i \hat{n}_i^b (\hat{n}_i^b - 1), \end{aligned} \quad (3)$$

$$\hat{V}_{bf} = \hbar U_{bf} \sum_{i\sigma} \hat{n}_{i\sigma}^f \hat{n}_i^b + \hbar g \sum_i (\hat{f}_{i\uparrow}^\dagger \hat{f}_{i\downarrow}^\dagger \hat{b}_i + \text{H.c.}). \quad (4)$$

Here $\hat{f}_{i\sigma}$ and \hat{b}_i are annihilation operators for the fermionic atoms of spin σ and bosonic molecules at the i -th site, respectively. The corresponding number operators $\hat{n}_{i\sigma}^f$ and \hat{n}_i^b have eigenvalues $n_{i\sigma}^f$ and n_i^b . The conserved quantity

$$N_F^{\text{tot}} = 2 \sum_i n_i^b + \sum_{i\sigma} n_{i\sigma}^f \quad (5)$$

is the total number of fermions in the system.

The Hamiltonians \hat{H}_f and \hat{H}_b describe standard Hubbard models for fermions and bosons, respectively, and \hat{V}_{bf} describes the interactions between fermions and bosons. The terms proportional to J_α , where $\alpha = f, b$, account for the tunneling of particles between nearest neighbor sites denoted by $\langle ij \rangle$. The single-particle center-of-mass energies are $\hbar \omega_\alpha$, and the effective detuning between the Raman lasers and the difference in internal energies of the atoms and molecules is $\hbar \omega_d$. The on-site fermion-fermion, boson-boson, and boson-fermion collisions are described by the interaction strengths U_f , $U_b (> 0)$, and U_{bf} , respectively. Finally, the term proportional to g in \hat{V}_{bf} describes the conversion of fermionic atoms into bosonic molecules, and vice versa, via photoassociation.

We concentrate on the case where the system consists initially of bosonic molecules only, and the corresponding initial state is the ground state of the Bose-Hubbard Hamiltonian \hat{H}_b . It is well-known that the ground state of this model describes either a MI phase or a SF phase, depending on the ratio U_b/zJ_b , where z is a number of nearest neighbor sites, for a fixed number of bosons [21, 22, 23, 24, 25, 26].

In the following we consider a strongly confining regime $|U_f| \gg zJ_f$. In this regime, Fermi pair states, that is, pairs of fermions with spins up and down occupying the same site, see upper diagrams in Fig. 1, have an energy separation U_f compared to unpaired states such as in the lower diagram. This allows us to treat the fermionic tunneling that couples the paired and unpaired states perturbatively. Since in addition the photodissociation of a molecule always creates a Fermi pair at a given lattice site, the unpaired states can then be adiabatically eliminated and integrated out. This results in the tunneling of Fermi pairs via those virtual states (Fig. 1), and the Hamiltonian \hat{H}_f is mapped on a pseudo-spin-1/2 system (XXZ model) by second-order degenerate perturbation theory [18, 27],

$$\hat{H}_s = \hbar \omega_s \sum_i (2\hat{s}_{fi}^z + 1) + \frac{\hbar J_s}{2} \sum_{\langle ij \rangle} (\hat{s}_{fi}^+ \hat{s}_{fj}^- + \hat{s}_{fi}^- \hat{s}_{fj}^+ - 2\hat{s}_{fi}^z \hat{s}_{fj}^z). \quad (6)$$

Here $\omega_s = \omega_f + U_f/2$ and $J_s = 4J_f^2/U_f$, and we have introduced the pseudo-spin operators describing the creation and annihilation of a Fermi pair

$$\hat{s}_{fi}^+ = \hat{f}_{i\uparrow}^\dagger \hat{f}_{i\downarrow}^\dagger, \quad \hat{s}_{fi}^- = \hat{f}_{i\downarrow} \hat{f}_{i\uparrow} \quad (7)$$

and

$$\hat{s}_{fi}^z = \frac{1}{2} (\hat{n}_{i\uparrow}^f + \hat{n}_{i\downarrow}^f - 1) \quad (8)$$

at the i -th site [28]. This mapping amounts to describing fermionic pairs as “effective two-level atoms” whose upper level corresponds to a pair of fermions, and lower level the absence of such a pair. Thus the presence of paired states at the i -th site is described by the spin-up state $|\hat{s}_{fi}^z = 1/2\rangle$ and its absence by the spin-down

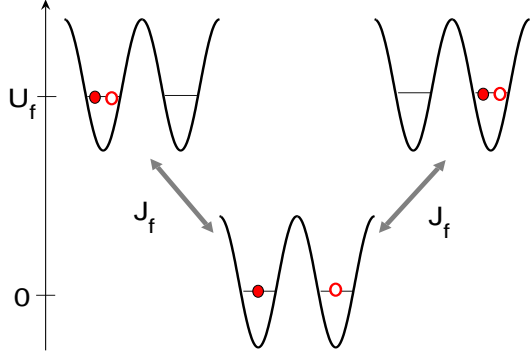


FIG. 1: (Color online) Schematics of the tunneling of a Fermi pair in the limit $U_f \gg zJ_f$. Filled and open circles present fermions with different spins.

state $|\hat{s}_{fi}^z = -1/2\rangle$. The pseudo-spin operators obey the commutation relations

$$[\hat{s}_{fi}^z, \hat{s}_{fj}^\pm] = \pm \hat{s}_{fi}^\pm \delta_{i,j}, \quad [\hat{s}_{fi}^+, \hat{s}_{fj}^-] = 2\hat{s}_{fi}^z \delta_{i,j}.$$

In terms of these operators the interaction Hamiltonian \hat{V}_{bf} can be re-expressed as

$$\hat{V}_{sb} = \hbar U_{bf} \sum_i (2\hat{s}_{fi}^z + 1) \hat{n}_i^b + \hbar g \sum_i (\hat{b}_i^\dagger \hat{s}_{fi}^- + \hat{s}_{fi}^+ \hat{b}_i). \quad (9)$$

We thus conclude that in the strongly confining regime the dissociation of initially bosonic molecular states into fermionic atoms is governed by the spin-boson lattice Hamiltonian [18]

$$\hat{H}_{SB} = \hat{H}_s + \hat{H}_b + \hat{V}_{sb}. \quad (10)$$

This effective Hamiltonian is valid for both of attractive and repulsive fermion-fermion interaction cases for the problem at hand.

B. Gutzwiller mean-field ansatz

In order to proceed we now introduce a Gutzwiller-type (GW) variational ansatz [22, 23] for the many-body wave function as

$$|\Psi(t)\rangle = \prod_{i=1}^{N_s} \left(\sum_{n_i=0}^{\infty} \sum_{s_i=-1/2}^{1/2} f_{n_i, s_i}^{(i)}(t) |n_i\rangle_b \otimes |s_i\rangle_{fp} \right), \quad (11)$$

where N_s is the number of lattice sites, and $|n_i\rangle_b$ and $|s_i\rangle_{fp}$ refer to number states of the bosons and Fermi pair at the i -th site, respectively. The normalization condition $\sum_{n_i, s_i} |f_{n_i, s_i}^{(i)}(t)|^2 = 1$ is satisfied at every single site. From the time-dependent variational principle, the time evolution of the variational parameters $f_{n_i, s_i}^{(i)}$ is obtained via the minimization

$$\frac{\partial}{\partial f_{n_i, s_i}^{(i)*}} \left\langle \Psi(t) \left| i\hbar \frac{\partial}{\partial t} - \hat{H}_{SB} \right| \Psi(t) \right\rangle = 0. \quad (12)$$

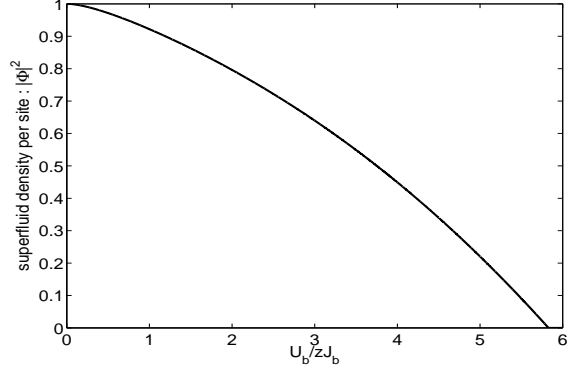


FIG. 2: Superfluid density $|\Phi|^2$ of the molecular ground state as a function of U_b/zJ_b . The MI-SF critical point is at about 5.83.

The time-dependent Gutzwiller approach has previously been used in the studies of several ultracold systems on lattices, such as bosonic atomic-molecular gases [29, 30], disorder [31], inhomogeneous [32] Bose-Hubbard systems and non-resonant Bose-Fermi mixtures [33]. In all cases the time dependence of the system parameters was assumed to be slow enough that the system is allowed to evolve adiabatically.

In the present case, the ground state of the bosonic molecules in the absence of photoassociation is given by the stationary solution of Eq.(12) with $f_{n_i, 1/2}^{(i)} = 0$ and $g = 0$. One of the merits of the Gutzwiller ansatz is its prediction of the MI-SF phase transition for a commensurate filling factor. For a fixed number of bosonic molecules, the ground state is determined by the single parameter U_b/zJ_b and the corresponding configuration of $\{f_{n_i, -1/2}^{(i)}\}$ is uniform over all lattice sites. At $U_b = 0$, corresponding to the deep SF regime, the ground state is a coherent state and the variation parameters for the system for the filling factor ν are given by

$$f_{n_i, -1/2}^{(i)} = e^{-\nu/2} \frac{(\sqrt{\nu})^{n_i}}{\sqrt{n_i!}}, \quad (13)$$

leading to Poissonian number statistics at each site. For a finite U_b the ground-state number statistics of molecules becomes subpoissonian, and in the MI phase, $U_b/zJ_b \gtrsim 5.83$ for $\nu = 1$, it becomes a Fock state $f_{n_i, -1/2}^{(i)} = \delta_{n_i, \nu}$. Fig. 2 shows the superfluid density per site $|\Phi|^2$ of the molecular ground state, as a function of U_b/zJ_b for the commensurate case $\nu = 1$, where $\Phi = \langle \hat{b}_i \rangle$.

It can be shown from the minimization of Eq. (12) that the resulting variational parameters $\{f_{n_i, s_i}^{(i)}\}$ remain uniform over the entire lattice when starting from a uniform configuration. This is the case for the dissociation of ground-state bosonic molecules. In that case the equations of motion for the site-independent parameters

$\{f_{n,s}\}$ are found to be

$$\begin{aligned} i\frac{\partial f_{n,s}}{\partial t} = & h_{n,s}f_{n,s} + g[\sqrt{n}f_{n-1,s+1} + \sqrt{n+1}f_{n+1,s-1}] \\ & - zJ_b[\sqrt{n+1}\Phi^*f_{n+1,s} + \sqrt{n}f_{n-1,s}\Phi] \\ & + \frac{zJ_s}{2}[\Delta^*f_{n,s+1} + f_{n,s-1}\Delta - 2sMf_{n,s}], \end{aligned} \quad (14)$$

where $h_{n,s} = \delta n + (U_b/2)n(n-1) + U_{bf}n(2s+1)$ and $\delta = \omega_d + \omega_b - 2\omega_s$. Here, we have used the average number conservation

$$\begin{aligned} N_F^{\text{tot}} = & 2N_m = 2\sum_i \left(\langle \hat{n}_i^b \rangle + \langle \hat{s}_{fi} \rangle + \frac{1}{2} \right) \\ = & 2N_s \left\{ \sum_{n,s} \left(n + s + \frac{1}{2} \right) |f_{n,s}|^2 \right\} \end{aligned} \quad (15)$$

and N_m is the initial number of molecules. We have also introduced the superfluid order parameters of the molecular bosons, Φ , and the atomic Fermi pairs, Δ , and the magnetization M of the pseudo-spin as

$$\begin{aligned} \Phi(t) &\equiv \langle \hat{b}_i \rangle = \sum_{n,s} \sqrt{n+1}f_{n,s}^*f_{n+1,s}, \\ \Delta(t) &\equiv \langle \hat{f}_{i\downarrow}\hat{f}_{i\uparrow} \rangle = \langle \hat{s}_{fi}^- \rangle = \sum_{n,s} f_{n,s}^*f_{n,s+1}, \\ M(t) &\equiv \langle \hat{s}_{fi}^z \rangle = \sum_{n,s} s|f_{n,s}|^2. \end{aligned}$$

Note that in Eq. (14), the tunneling of both bosons and Fermi pairs occurs only via their own order parameters, and fluctuations about their mean values are ignored. In this sense, the GW ansatz can be thought of as a kind of mean-field approximation.

III. LIMITING CASES

Before turning to the presentation of a numerical study of Eq.(14), we first discuss analytical results for the dissociation dynamics in several limiting cases that provide us with some useful intuitive understanding of its behavior.

A. Generalized Jaynes-Cummings dynamics : $zJ_b, zJ_s \ll g$

In the limit $J_b, J_s \rightarrow 0$, the spin-boson Hamiltonian \hat{H}_{SB} reduces to a generalized version of Jaynes-Cummings (J-C) model [34] at each lattice site. This situation can be solved exactly [28]. The average number of molecules per site, n_b , is

$$n_b(t) = \sum_n p(n) \frac{4g^2n}{\mathcal{R}_{n-1}^2} \cos^2 \left(\frac{\mathcal{R}_{n-1}t}{2} \right), \quad (16)$$

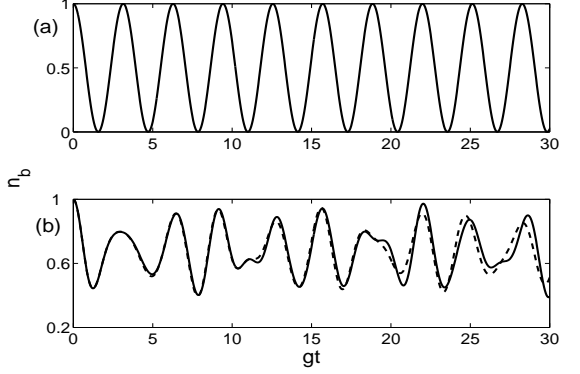


FIG. 3: Time evolution of the average molecule number per site n_b according to the Jaynes-Cummings dynamics for initially (a) a number state corresponding to the Mott-Insulator phase and (b) a coherent state. Both situations are for $U_{bf} = 0$ and exact resonance $\delta = 0$, and for $\nu = 1$. The dashed line is the GW mean-field solution for $zJ_b/g = 0.1$.

where the Rabi frequency \mathcal{R}_n ,

$$\mathcal{R}_n = \sqrt{\{\delta + (U_b - 2U_{bf})n\}^2 + 4g^2(n+1)}, \quad (17)$$

depends on the number n of molecules. In Eq. (16), $p(n) = |f_{n-1/2}(t=0)|^2$ is the initial number statistics of the molecules at each lattice site. We note that the GW mean-field equation (14) has the same exact solution and thus describes the correct dynamics in this limit.

The time evolution of n_b at exact resonance, $\delta = 0$ for a molecular field initially in the MI phase ($U_b \gg zJ_b$) and the superfluid phase ($U_b = 0$) is shown in Fig. 3 (a) and Fig. 3 (b), respectively, for the filling factor $\nu = N_m/N_s = 1$. In this example we have taken $U_{bf} = 0$. Note also that the on-site interaction between atoms and molecules plays no role in the dynamics starting from the MI state for $\nu = 1$. The dashed line in Fig. 3 (b), obtained from Eq. (14) for small but finite tunneling, $zJ_b/g = 0.1$, illustrates the small deviation from the Jaynes-Cummings solution (16) in that case.

These results demonstrate that the observation of the number of atoms, which is the difference between the total number of fermions and twice the molecule number and is easier to observe than that of number of molecules, can reveal the precise number statistics of the molecules and hence their ground-state properties. A similar argument was previously given by K. Mølmer in the context of bosonic atom-molecule gases in an optical lattice [35].

B. Generalized Tavis-Cummings dynamics : $zJ_b \gg g$ and $U_b/zJ_b \lesssim 1$

As shown in Fig. 2, for $U_b/zJ_b \lesssim 1$ the initial molecular ground state contains a large condensate fraction or high occupation of the zero-momentum state. Moreover, the

application of a weak photoassociation coupling, $zJ_b \gg g$, presumably preserves the coherent character of the molecular condensate. Owing to Bose enhancement, in that limit the dissociation dynamics is therefore expected to be dominated by the condensate of bosonic molecules.

Assuming $J_s = 0$ for simplicity, the momentum representation of the Hamiltonian (10) is

$$\begin{aligned} \hat{H}_{SB} = & \sum_{\mathbf{k}} \left[\hbar\omega_{\mathbf{k}} \hat{b}_{\mathbf{k}}^\dagger \hat{b}_{\mathbf{k}} + \frac{\hbar g}{\sqrt{N_s}} \sum_i \left(e^{i\mathbf{k}\mathbf{r}_i} \hat{b}_{\mathbf{k}}^\dagger \hat{s}_{fi}^- + \text{H.c.} \right) \right] \\ & + \frac{\hbar U_{bf}}{N_s} \sum_{\mathbf{k}_1, \mathbf{k}_2} \sum_i e^{i(\mathbf{k}_1 - \mathbf{k}_2)\mathbf{r}_i} \hat{b}_{\mathbf{k}_1}^\dagger \hat{b}_{\mathbf{k}_2} (2\hat{s}_{fi}^z + 1) \\ & + \frac{\hbar U_b}{2N_s} \sum_{\mathbf{k}_1, \mathbf{k}_2} \sum_{\mathbf{k}_3, \mathbf{k}_4} \delta_{\mathbf{k}_1 + \mathbf{k}_2, \mathbf{k}_3 + \mathbf{k}_4} \hat{b}_{\mathbf{k}_1}^\dagger \hat{b}_{\mathbf{k}_2}^\dagger \hat{b}_{\mathbf{k}_3} \hat{b}_{\mathbf{k}_4} \end{aligned} \quad (18)$$

where $\hat{b}_{\mathbf{k}}$ is the annihilation operator of the bosonic molecules with momentum \mathbf{k} and \mathbf{r}_i is the coordinate of site i . The single-molecule frequency for a regular lattice of lattice constant a in d dimensions is given by

$$\omega_{\mathbf{k}} = \delta - 2J_b \sum_{j=1}^d \cos(k_j a).$$

In the extreme superfluid case, the non-condensed molecule fraction is negligible and a single-mode approximation that accounts only for the zero-momentum state is appropriate. The replacement $\hat{b}_{\mathbf{k}} \rightarrow \hat{b}_0$, together with the approximate number conservation

$$N_m = \hat{n}_0 + \sum_i (\hat{s}_{fi}^z + 1/2), \quad (19)$$

where $\hat{n}_0 = \hat{b}_0^\dagger \hat{b}_0$, simplifies then the Hamiltonian (18) to a generalized version of the Tavis-Cummings (T-C) model of quantum optics [36]

$$\hat{H}_0 \rightarrow \hbar\delta_0 \hat{n}_0 + \frac{\hbar g}{\sqrt{N_s}} \left[\hat{b}_0^\dagger \hat{S}_f^- + \text{H.c.} \right] + \frac{\hbar U_0}{2N_s} \hat{n}_0^2. \quad (20)$$

Here $\hat{S}_f = \sum_i \hat{s}_{fi}$ is a collective spin operator over the entire lattice, and the effective detuning and effective interaction strength are now

$$\delta_0 = \delta - zJ_b + 2\nu U_{bf}, \quad U_0 = U_b - 4U_{bf},$$

where we have neglected a term of $\mathcal{O}(1/N_s)$. As a result of the absence of the phase factor $e^{i\mathbf{k}\mathbf{r}_i}$ for the zero-momentum condensate molecules in the conversion term of \hat{H}_0 , the system undergoes cooperative oscillations between atoms and molecules. Similar models have been applied to the atom-molecule dynamics across the BCS-BEC crossover [37, 38] and the dissociation dynamics of a molecular BEC [39] in free space.

Although the Hamiltonian (20) can be solved numerically by direct diagonalization, it is useful to consider an approximate analytical solution valid in the semiclassical limit [40]. By treating the molecule number operator $\hat{n}_0 \rightarrow n_0$ classically and taking into account number

conservation (19) and energy conservation, we can recast the Tavis-Cummings dynamics in the form of a Newton equation

$$\frac{d^2}{dt^2} n_0(t) = -\frac{d}{dn_0} V(n_0), \quad (21)$$

where the potential $V(n)$ is given by [40]

$$\begin{aligned} V(n) = & \frac{U_0^2}{8N_s^2} n^4 + \left\{ \frac{2g^2}{N_s} + \frac{\delta_0 U_0}{2N_s} \right\} n^3 \\ & - \left\{ 4g^2 \left(\nu - \frac{1}{2} \right) - \frac{\delta_0^2}{2} + \frac{\delta_0 U_0 \nu}{2} + \frac{U_0^2 \nu^2}{4} \right\} n^2 \\ & - \left\{ 2g^2 (1 - \nu) + \delta_0^2 + \frac{\delta_0 U_0 \nu}{2} \right\} N_m n. \end{aligned} \quad (22)$$

In the case $U_0 = 0$, the potential is a cubic function of n , and $n_0(t)$ is given in terms of the Jacobian elliptic function $\text{sn}(\theta; k)$ [41] as

$$\frac{n_0(t)}{N_m} = 1 - (1 - n_+) \text{sn}^2 \left(\sqrt{(1 - n_-) \nu} gt; k \right), \quad (23)$$

where

$$\begin{aligned} n_{\pm} = & \frac{1}{2\nu} \left[- \left\{ \left(\frac{\delta_0}{2g} \right)^2 - \nu + 1 \right\} \right. \\ & \left. \pm \sqrt{\left\{ \left(\frac{\delta_0}{2g} \right)^2 - \nu + 1 \right\}^2 + 4\nu \left(\frac{\delta_0}{2g} \right)^2} \right], \end{aligned}$$

and $k = \sqrt{(1 - n_+)/(1 - n_-)}$.

For $\delta_0 = 0$, the classical trajectory approaches an unstable equilibrium point at $n_0 = 0$ when $\nu = 1$ [38]. It can be shown from Eq. (23) that $\nu \neq 1$ excludes the presence of unstable extremum. For large detunings, $\delta_0/2g \gg \sqrt{\nu}, 1$, the oscillations become sinusoidal

$$\frac{n_0(t)}{N_m} \rightarrow 1 - \left(\frac{2g}{\delta_0} \right)^2 \sin^2 \left(\frac{\Omega t}{2} \right), \quad (24)$$

where

$$\Omega \approx \sqrt{\delta_0^2 + 4(1 + \nu)g^2}. \quad (25)$$

Figure 4 shows the time evolution of n_b for $\delta_0/g = -1$, $U_b = U_{bf} = 0$, and $\nu = 1$. The solid and dashed lines are the semiclassical and quantum-mechanical Tavis-Cummings solutions, respectively, for $N_m = 2000$ and $n_b = n_0$. The GW mean-field solution (dot-dashed line for $zJ_b/g = 20$) is seen to agree quantitatively with the Tavis-Cummings dynamics in the limit $zJ_b \gg g$ for $U_b/zJ_b \lesssim 1$.

IV. GUTZWILLER MEAN-FIELD DYNAMICS

The preceding section illustrated in limiting cases the crossover of the dissociation dynamics from a regime of

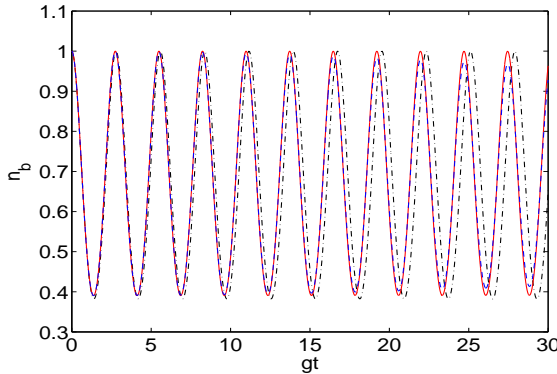


FIG. 4: (Color online) Time evolution of n_b for $\delta_0/g = -1$, $U_b = U_{bf} = 0$, and $\nu = 1$. The solid and dashed lines correspond to the semiclassical and quantum ($N_m = 2000$) solutions of the Tavis-Cummings dynamics, respectively, and the dot-dashed line is the GW mean-field solution for $zJ_b/g = 20$.

independent single-site dynamics to a regime of cooperative dynamics as the molecular tunneling is increased. In this section we examine the characteristics of the dissociation in these regimes in more detail within the framework of a Gutzwiller ansatz. We also demonstrate the appearance of two types of self-trapping transitions, depending on the ratio U_b/zJ_b . We restrict our discussion to the case $J_s = U_{bf} = 0$ and to the commensurate case $\nu = 1$ for simplicity. The effects of the XXZ term proportional to J_s in the Hamiltonian \hat{H}_s are briefly discussed in the last subsection.

A. Crossover between single-site and cooperative dynamics

Figure 5 shows a schematic phase diagram summarizing the characteristics of the GW dynamics in the U_z/g - zJ_b/g plane. For $zJ_b \gg g$ and $U_b/zJ_b \lesssim 1$, the dynamics is dominated by the molecular condensate and hence cooperative. In the opposite limit, $zJ_b \ll g$, the dynamics on a given lattice site becomes increasingly independent of the other sites. Note that the thick gray lines in the figure do not indicate sharp boundaries between these regimes. The dashed line marks the separation between initial molecular ground states in the MI and SF phases. Note that for a molecular field initially in the MI phase ($U_b/zJ_b \gtrsim 5.83$), the full Rabi oscillation of Fig. 3a is always recovered at every single site since $\langle \hat{b}_i \rangle = 0$ in that case.

Figure 6 shows time evolution of the average number n_b of molecules (solid line), the superfluid density $|\Phi|^2$ of bosons (dashed line), and the order parameter $|\Delta|^2$ of Fermi pairs (dot-dashed line) per site for (a) $zJ_b/g = 0.1$, (b) $zJ_b/g = 1$, and (c) $zJ_b/g = 10$ and for $\delta = zJ_b$ and a fixed $U_b/zJ_b = 0.1$. The corresponding probabilities $|f_{n,s}|^2$ for these three regimes are shown in Fig. 7. The

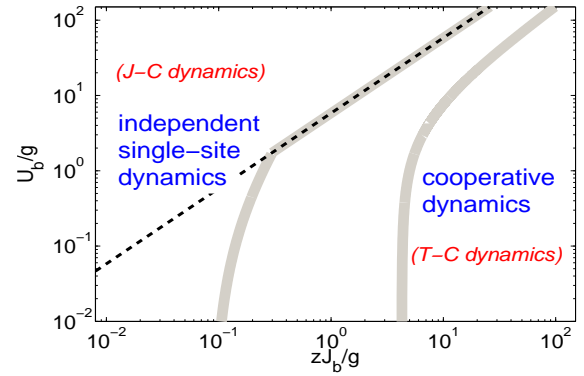


FIG. 5: (Color online) Phase diagram of the GW mean-field dynamics. The dashed line indicates the MI-SF phase transition for the initial molecular ground state.

initial molecular ground state is the same in all cases and corresponds to an almost coherent state.

In the case of weak tunneling, Fig. 6 (a), the system dynamics resembles the Jaynes-Cummings limit, see Fig. 3 (b): pairs of amplitudes, $f_{n-1,1/2}$ and $f_{n,-1/2}$, are coupled to each other but uncoupled to the other amplitudes. This is shown in Fig. 7 (a), where the probabilities of neighboring states, $(n, \text{sign}(s)) = (n-1, +)$ and $(n, -)$, oscillate at a frequency $\sim 2\sqrt{ng}$. In practice, however, each of those amplitudes is of course also weakly coupled to others due to finite tunneling. Note that the probability of the $(0, -)$ state remains almost constant at all times since it has no direct partner.

As zJ_b/g increases, the system dynamics becomes increasingly dominated by the molecular condensate component. In the extreme case of $zJ_b/g = 10$, we reach a regime of clear periodic motion between the molecular and atomic superfluids. Figures 7 (b) and (c) show that the Jaynes-Cummings character of Fig. 7 (a) disappears with increasing zJ_b/g , and a high degree of coherence develops, accompanied by the formation of new order characterized by the simultaneous appearance of several molecular number states of same spin.

B. Self-trapping transitions

In this subsection we examine how the dissociation dynamics is affected by the initial state of the molecular field, or stated another way, whether it undergoes a sudden transition as a function of U_b/zJ_b .

To answer this question we solved numerically the GW mean-field equations for several values of U_b/zJ_b for $zJ_b/g = 20$ and $\delta = 0$. Fig. 8 shows the time evolution of n_b (solid line), $|\Phi|^2$ (dashed line), and $|\Delta|^2$ (dot-dashed line) from (a) $U_b/zJ_b = 1.50$ to (f) $U_b/zJ_b = 5.50$. Since the initial superfluid fraction decreases as U_b/zJ_b increases, these results illustrate situations where the dissociation dynamics changes from being “coher-

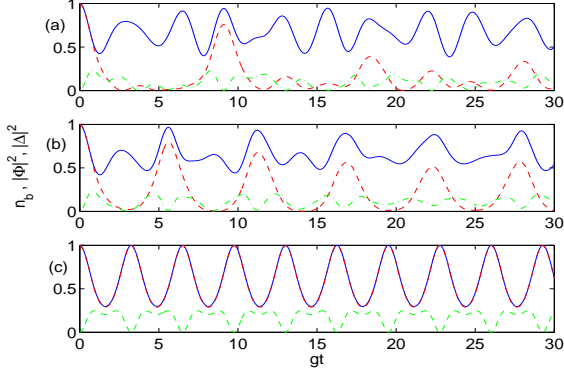


FIG. 6: (Color online) Time evolution of n_b (solid line), $|\Phi|^2$ (dashed line), and $|\Delta|^2$ (dot-dashed line) for (a) $zJ_b/g = 0.1$, (b) $zJ_b/g = 1$, and (c) $zJ_b/g = 10$, and for $\delta = zJ_b$, $U_b/zJ_b = 0.1$.

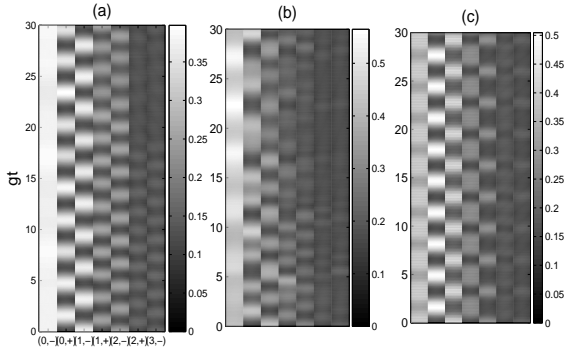


FIG. 7: Gray scale rendition of the time evolution of the probabilities $|f_{n,s}|^2$ of the states $(n, \text{sign}(s))$ for (a) $zJ_b/g = 0.1$, (b) $zJ_b = 1$, and (c) $zJ_b/g = 10$, respectively. The darker shades of gray indicate higher probabilities. Same parameters are taken as in Fig. 6.

ent”, or condensate-dominated, to “incoherent,” or non-condensate dominated. Interestingly, we find two types of transitions against small variations of U_b/zJ_b : the first one is a sudden suppression of the amplitude of oscillations between Figs. 8 (b), $U_b/zJ_b = 1.86$, and (c), $U_b/zJ_b = 1.87$; and the second is a sudden increase of that amplitude between Figs. 8 (d), $U_b/zJ_b = 4.70$, and (e), $U_b/zJ_b = 4.71$. Such a transition from a small amplitude oscillation (localized solution) to a large amplitude oscillation (delocalized solution), and vice versa, due to a nonlinearity of the system is known as a self-trapping transition [15, 16]. Since these two transitions have very different coherence properties, we refer to them from now on as the *coherent* self-trapping transition for the former and the *incoherent* self-trapping transition for the latter, respectively.

The Tavis-Cummings model of Sec. III provides a useful way to understand why two different self-trapping

transitions are present against a variation of U_b/zJ_b . If we regard the third term in Eq. (20), corresponding to the molecule-molecule interaction, as a nonlinear detuning, the energy difference between number states of n condensate bosons and $n - 1$ condensate bosons is given by $\hbar\Omega_n = \hbar\delta_0 + \hbar U_0(n/N_s)$ where we have neglected a term of order $1/N_s$. The dynamical properties are determined by the competition between that detuning and the photoassociation term in Eq. (20). When the detuning is dominant the dynamics is characterized by small amplitude oscillations, while large amplitude oscillations appear when the atom-molecule coupling is dominant. In the intermediate region where these two effects are comparable, that is, for $\Omega_n \sim g$, a self-trapping transition appears. Replacing n/N_s in the nonlinear detuning energy Ω_n by the initial superfluid density of bosons per site, $|\Phi(t = 0; U_b/zJ_b)|^2$ which depends on the ratio of U_b/zJ_b as shown in Fig. 2, we obtain, for $\delta = 0$ and $U_{bf} = 0$,

$$\Omega_n = -zJ_b + U_b|\Phi(t = 0; U_b/zJ_b)|^2$$

This frequency becomes equal to zero for two values of U_b/zJ_b . For large values of zJ_b/g , such as in Figs. 8, self-trapping transitions occur around at these two resonance points.

Self-trapping transitions can also be understood in a different picture from the semiclassical form (21) of the generalized Tavis-Cummings Hamiltonian, which describes the motion of a classical particle in the potential $V(n_0)$ (22). At $t = 0$, the particle is at rest and is located at some point $n_0 = |\Phi(t = 0)|^2$ on the potential. Under the influence of the dissociation laser it then starts rolling down the potential $V(n_0)$ toward smaller values of n_0 , passes through a potential minimum, and moves uphill up to a point having the same potential energy as initially. At this point the particle turns back, resulting in periodic oscillations in the (continuous) molecule number. What happens near the self-trapping condition is that an additional potential barrier appears in the potential. For delocalized (resp. localized) solutions, the particle can (resp. cannot) climb up the barrier, resulting in a sudden transition between large and small amplitude oscillations. The key factor in achieving this transition is the quartic form of the potential $V(n_0)$, which disappears in the absence of the effective two-body interaction U_0 [40].

This classical interpretation relies on the assumption that the dynamics of the condensate fraction is uncoupled to that of the non-condensate component. Since the GW variational state also involves a non-condensate component, the corresponding mean-field solutions are expected to deviate somewhat from those of Eq. (21), especially in the vicinity of the *incoherent* self-trapping critical point. Figure 9 shows the critical curve of the self-trapping transitions in the $U_b/zJ_b - zJ_b/g$ plane for $\delta = 0$. The dashed line corresponds to the semiclassical solution of the Tavis-Cummings dynamics, obtained by replacing $\nu \rightarrow \nu_0 = |\Phi(t = 0)|^2$ in the potential $V(n_0)$. The

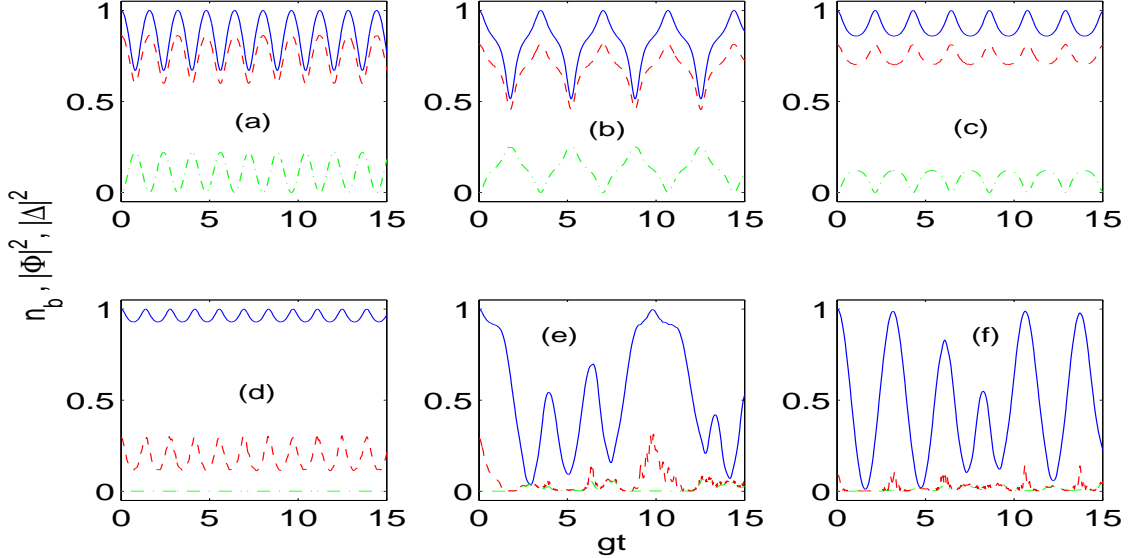


FIG. 8: (Color online) Time evolution of n_b (solid line), $|\Phi|^2$ (dashed line), and $|\Delta|^2$ (dot-dashed line) for $zJ_b/g = 20$, $\delta = 0$, and for (a) $U_b/zJ_b = 1.50$ (b) $U_b/zJ_b = 1.86$, (c) $U_b/zJ_b = 1.87$, (d) $U_b/zJ_b = 4.70$, (e) $U_b/zJ_b = 4.71$, and (f) $U_b/zJ_b = 5.50$.

stars are mean-field results obtained by seeking a point where a sudden suppression of amplitude happens in the first oscillation period [42]. Both these results have a C shape, with localized solutions present inside the curve, and share several common features: first, we observe that two transitions occur for a given zJ_b/g . They correspond to *coherent*, respectively *incoherent* transitions, for the lower and upper values of U_b/zJ_b . Second, the transitions disappear below some value of zJ_b/g .

In the vicinity of the *incoherent* transition, the mean-field dynamics of the delocalized solutions is very different from its semiclassical counterpart. As shown in Fig. 8(e), a large incoherent oscillation occurs once the molecular condensate reaches a sufficiently small value, indicating that the delocalization in the motion of molecular condensate is a trigger for an incoherent large amplitude oscillation in the system. This region is also characterized by large fluctuations

$$\sigma_b = \sqrt{\frac{\langle (\hat{n}_i^b)^2 \rangle - \langle \hat{n}_i^b \rangle^2}{\langle \hat{n}_i^b \rangle}},$$

in the molecule number fluctuations, a feature that is of course ignored in the semiclassical description. Fig. 10 shows the time evolution of σ_b for the cases of Fig. 8 (d) (dashed line), and (e) (solid line).

C. Intersite spin-spin coupling

Finally, we briefly discuss the effects of XXZ term in the Hamiltonian \hat{H}_s . It is known that the trap frequencies of homonuclear molecules in a lattice site almost coincide with the atomic trap frequencies [7, 14], so that in

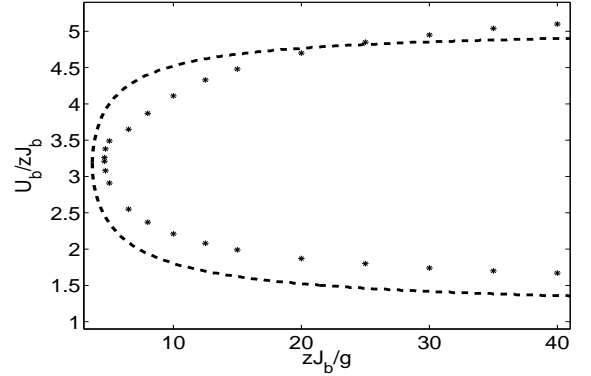


FIG. 9: Critical curve of the self-trapping transitions. The star and dashed lines are for the GW mean-field and the semiclassical Tavis-Cummings solutions, respectively. The inside of the curve is the domain of localized solutions.

general $J_f \gg J_b$ due to the higher mass of the molecules, $m_b = 2m_f$. However, if the inequality $|U_f| \gg zJ_f$ that underlies all of the considerations in this paper is fulfilled, the effective tunneling of the fermions is given by $J_s = 4J_f^2/U_f$, which can then easily lead to a system of $|J_s| \leq J_b$ where the intersite spin-spin coupling does not affect the coherence properties of the dynamics. In the following we limit our considerations to this case [43].

In the regime of cooperative dynamics of Fig. 5, the spin-spin coupling gives rise to a positive (resp. negative) detuning effect for the case of attractive (resp. repulsive) fermion-fermion interaction, since a superfluid state of Fermi pairs ($|\Delta| \neq 0$) lowers, resp. raises the energy for $U_f < 0$, resp. $U_f > 0$. This additional detuning

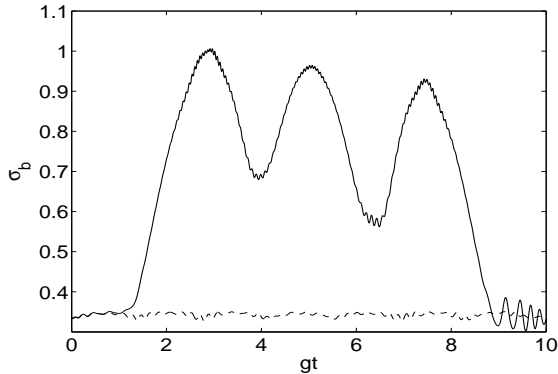


FIG. 10: Molecule number fluctuations per site, σ_b , across the *incoherent* self-trapping transition point for the cases of Fig. 8 (d) (dashed line) and (e) (solid line).

can however be compensated by changing the photodissociation detuning energy δ . We have checked that finite values of J_s preserve the appearance of the self-trapping transitions. Finally, in the regime of incoherent dynamics the effects of the XXZ term become weaker with decreasing zJ_b/g . We thus conclude that the discussion in the preceding subsections holds even in the presence of the intersite spin-spin coupling.

V. SUMMARY

In this paper we have investigated theoretically the photodissociation of ground-state bosonic molecules into

two-component fermionic atoms in an optical lattice. We showed that the dissociation dynamics in the strong fermion-fermion interaction limit, $|U_f| \gg zJ_f$, is governed by a spin-boson lattice Hamiltonian dynamics. Using a Gutzwiller mean-field analysis, we examined the crossover of the dissociation dynamics from an independent single-site regime to a cooperative regime as the molecular tunneling is increased. We also showed the appearance of two types of transitions, that is *coherent* and *incoherent* self-trapping transitions, as a small variation of U_b/zJ_b . The mean-field approximation only accounts for those tunnel processes proportional to the expectation values of bosonic and fermionic pair operators. Thus, when starting from the MI molecular phase the dynamics of the atoms and molecules inside the individual lattice sites always remains independent of the other sites. In this situation, genuine quantum effects are significant, and are closely related to the stability of the MI phase under boson-fermion conversion [19] and to the formation of SF correlations across the MI-SF critical point [6]. This will be discussed in a future publication.

Acknowledgments

This work is supported in part by the US Office of Naval Research, by the National Science Foundation, by the US Army Research Office, and by the National Aeronautics and Space Administration.

[1] S. Inouye, M. R. Andrews, J. Stenger, H.-J. Miesner, D. M. Stamper-Kurn, and W. Ketterle, *Nature* (London) **392**, 151 (1998).
[2] R. Wynar, R. S. Freeland, D. J. Han, C. Ryu, and D. J. Heinzen, *Science* **287**, 1016 (2000).
[3] D. Jaksch and P. Zoller, *Ann. Phys.* **315**, 52 (2005).
[4] I. Bloch, *J. Phys. B: At. Mol. Opt.* **38**, S629 (2005).
[5] J. Dziarmaga, A. Smerzi, W. H. Zurek, and A. R. Bishop, *Phys. Rev. Lett.* **88**, 167001 (2002); B. Damski, *ibid.* **95**, 035701 (2005); W. H. Zurek, U. Dorner, and P. Zoller, *ibid.*, 105701 (2005); J. Dziarmaga, *ibid.*, 245701 (2005); A. Polkovnikov, *Phys. Rev. B* **72**, 161201(R) (2005).
[6] K. Sengupta, S. Powell, and S. Sachdev, *Phys. Rev. A* **69**, 053616 (2004); F. M. Cucchietti, B. Damski, J. Dziarmaga, and W. H. Zurek, e-print cond-mat/0601650.
[7] T. Rom, T. Best, O. Mandel, A. Widera, M. Greiner, T. W. Hänsch, and I. Bloch, *Phys. Rev. Lett.* **93**, 073002 (2004).
[8] M. Köhl, H. Moritz, T. Stöferle, K. Günter, and T. Esslinger, *Phys. Rev. Lett.* **94** 080403 (2005).
[9] R. B. Diener and T. L. Ho, *Phys. Rev. Lett.* **96**, 010402 (2006).
[10] T. Stöferle, H. Moritz, K. Günter, M. Köhl, and T. Esslinger, *Rhys. Rev. Lett.* **96**, 030401 (2006).
[11] T. Busch, B.-G. Englert, K. Rzazewski, and M. Wilkends, *Found. Phys.* **28**, 549 (1998).
[12] D. Blume and C. H. Greene, *Phys. Rev. A* **65**, 043613 (2002).
[13] G. Thalhammer, K. Winkler, F. Lang, S. Schmid, R. Grimm, and J. H. Denschlag, *Phys. Rev. Lett.* **96**, 050402 (2006).
[14] C. Ryu, X. Du, E. Yesilada, A. M. Dudarev, S. Wan, Q. Niu, and D. J. Heinzen, e-print cond-mat/0508201.
[15] G. J. Milburn, J. Corney, E. M. Wright, and D. F. Walls, *Phys. Rev. A* **55**, 4318 (1997).
[16] A. Smerzi, S. Fantoni, S. Giovanazzi, and S. R. Shenoy, *Phys. Rev. Lett.* **79**, 4950 (1997).
[17] D. B. M. Dickerscheid, U. Al Khawaja, D. van Oosten, and H. T. C. Stoof, *Phys. Rev. A* **71**, 043604 (2005).
[18] L. D. Carr and M. J. Holland, *Phys. Rev. A* **72**, 031604(R) (2005).
[19] F. Zhou, *Phys. Rev. B* **72**, 220501(R) (2005); F. Zhou and C. Wu, e-print cond-mat/0511589.
[20] T. Miyakawa and P. Meystre, *Phys. Rev. A* **73**, 021601(R) (2006).
[21] M. P. A. Fisher, P. B. Weichman, G. Grinstein, and

D. S. Fisher, Phys. Rev. B **40**, 546 (1989).

[22] D. S. Rokhsar and B. G. Kotliar, Phys. Rev. B **44**, 10328 (1991).

[23] W. Krauth, M. Caffarel, and J-P. Bouchaud, Phys. Rev. B **45**, 3137 (1992).

[24] S. Sachdev, *Quantum Phase Transitions* (Cambridge University Press, New York, 1999).

[25] D. Jaksch, C. Bruder, J. I. Cirac, C. W. Gardiner, and P. Zoller, Phys. Rev. Lett. **81**, 3108 (1998).

[26] M. Greiner, O. Mandel, T. Esslinger, T. W. Hänsch, and I. Bloch, Nature (London) **415**, 39 (2002).

[27] V. J. Emery, Phys. Rev. B **14**, 2989 (1976).

[28] C. P. Search, W. Zhang, and P. Meystre, Phys. Rev. Lett. **91**, 190401 (2003).

[29] D. Jaksch, V. Venturi, J. I. Cirac, C. J. Williams, and P. Zoller, Phys. Rev. Lett. **89**, 040402 (2002).

[30] B. Damski, L. Santos, E. Tiemann, M. Lewenstein, S. Kotochigova, P. Juliene, and P. Zoller, Phys. Rev. Lett. **90**, 110401 (2003).

[31] B. Damski, J. Zakrzewski, L. Santos, P. Zoller, and M. Lewenstein, Phys. Rev. Lett. **91**, 080403 (2003).

[32] J. Zakrzewski, Phys. Rev. A **71**, 043601 (2005).

[33] H. Fehrmann, M. A. Baranov, B. Damski, M. Lewenstein, and L. Santos, e-print cond-mat/0307635.

[34] M. O. Scully and M. S. Zubairy, *Quantum Optics* (Cambridge University Press, Cambridge, U.K., 1997).

[35] K. Mølmer, Phys. Rev. Lett. **90** 110403 (2003).

[36] M. Tavis and F. W. Cummings, Phys. Rev. **170**, 379 (1968).

[37] J. Javanainen, M. Koštrun, Y. Zheng, A. Carmichael, U. Shrestha, P. J. Meinel, M. Mackie, O. Dannenberg, and K-A. Suominen, Phys. Rev. Lett. **92**, 200402 (2004); R. A. Barankov and L. S. Levitov, *ibid.* **93**, 130403 (2004); A. V. Andreev, V. Gurarie, and L. Radzihovsky, *ibid.* **93**, 130402 (2004); D. Meiser and P. Meystre, *ibid.* **94**, 093001 (2005); E. Pazy, I. Tikhonenkov, Y. B. Band, M. Fleischhauer, and A. Vardi, *ibid.* **95**, 170403 (2005).

[38] H. Uys, T. Miyakawa, D. Meiser, and P. Meystre, Phys. Rev. A **72**, 053616 (2005).

[39] M. W. Jack and H. Pu, Phys. Rev. A **72**, 063625 (2005).

[40] T. Miyakawa and P. Meystre, Phys. Rev. A **71**, 033624 (2005).

[41] H. Hancock, *Elliptic Integrals* (Dover, New York, 1917); *Handbook of Mathematical Functions*, edited by M. Abramowitz and I. A. Stegun (Dover, New York, 1972).

[42] For a smaller value of $zJ_b/g \lesssim 8$, the fluctuations are enhanced, leading to a situation where large amplitude oscillation shows up after several small amplitude oscillations. Here, we regard these solutions as localized (self-trapping) solutions

[43] In the case of a large J_s , an additional self-trapping transition originating from the intersite spin-spin coupling can be found even for $U_b = U_{bf} = 0$.